NeuroImage: Clinical 7 (2015) 297–305

Contents lists available at ScienceDirect

NeuroImage: Clinical

journal homepage: www.elsevier.com/locate/ynicl

# Increased cortical surface area and gyrification following long-term survival from early monocular enucleation

Krista R. Kelly [a,b], Kevin D. DeSimone [a,b], Brenda L. Gallie [c], Jennifer K.E. Steeves [a,b,c,*]

[a] Department of Psychology, York University, Toronto, Canada
[b] Centre for Vision Research, York University, Toronto, Canada
[c] Department of Ophthalmology and Visual Sciences, The Hospital for Sick Children, Toronto, Canada

ARTICLE INFO

*Article history:*
Received 24 September 2014
Received in revised form 26 November 2014
Accepted 29 November 2014
Available online 3 December 2014

*Keywords:*
Monocular enucleation
Morphological development
Early visual deprivation
Visual cortex
Brain plasticity
Hemisphere asymmetry

ABSTRACT

*Purpose:* Retinoblastoma is typically diagnosed before 5 years of age and is often treated by enucleation (surgical removal) of the cancerous eye. Here, we sought to characterize morphological changes of the cortex following long-term survival from early monocular enucleation.
*Methods:* Nine adults with early right-eye enucleation (≤48 months of age) due to retinoblastoma were compared to 18 binocularly intact controls. Surface area, cortical thickness, and gyrification estimates were obtained from $T_1$ weighted images and group differences were examined.
*Results:* Early monocular enucleation was associated with increased surface area and/or gyrification in visual (i.e., V1, inferior temporal), auditory (i.e., supramarginal), and multisensory (i.e., superior temporal, inferior parietal, superior parietal) cortices compared with controls. Visual cortex increases were restricted to the right hemisphere contralateral to the remaining eye, consistent with previous subcortical data showing asymmetrical lateral geniculate nucleus volume following early monocular enucleation.
*Conclusions:* Altered morphological development of visual, auditory, and multisensory regions occurs subsequent to long-time survival from early eye loss.


## 1. Introduction

Although some morphological and physiological aspects of the visual system are established prenatally, this system is far from mature and continues to develop into adolescence (e.g., Garey and de Courten, 1983; Huttenlocher and De Courten, 1987; for review see Daw, 2006). Studies on animals with postnatal monocular deprivation from lid suture and humans with congenital cataracts or strabismus show adverse effects during postnatal development on visual behaviour (e.g., Wiesel and Hubel, 1965; Ellemberg et al., 2000). Monocular deprivation from strabismus and anisometropia also leads to changes in the morphology of the human visual system, including reductions in grey matter concentration in lateral geniculate nuclei (LGN) (Barnes et al., 2010) and grey matter volume in visual cortex (Mendola et al., 2005). These findings suggest that it is imperative for the developing visual system to receive balanced binocular input for typical postnatal maturation. Although these forms of deprivation provide an excellent model for studying monocular deprivation, the brain nonetheless receives anomalous visual input from the deprived eye.

Here, we investigated morphological development of the cortex in adults who have experienced a more complete form of early monocular deprivation, surgical removal of one eye (monocular enucleation), due to retinoblastoma (cancer of the retina). Although retinoblastoma is rare, it accounts for 6% of all childhood cancers and generally occurs before 5 years of age (Broaddus et al., 2009a, b). Unilateral retinoblastoma has a high survival rate, and eye enucleation is the most frequent and effective treatment due to the aggressive nature of the tumour. Monocular enucleation at such a young age is likely to alter visual system development since half of the visual inputs are deafferented at a time when the brain is not fully mature.

Behavioural studies show that early-enucleated adults exhibit impairments in motion perception including motion-defined letter recognition and speed discrimination, and different patterns of oculomotor function compared to binocularly intact controls (Reed et al., 1991; Steeves et al., 2002; Kelly et al., 2013b). These data indicate a critical period for receiving balanced binocular input for the development of these visual abilities. However, unlike other forms of monocular deprivation such as strabismus or amblyopia, spatial form visual abilities such as contrast sensitivity/discrimination and global shape discrimination remains intact or is enhanced following early monocular enucleation (Nicholas et al., 1996; Steeves et al., 2004; Kelly et al., 2013b). Intact/enhanced spatial form vision suggests that altered development occurs in

* Corresponding author at: Department of Psychology and Centre for Vision Research, York University, 4700 Keele St, Toronto, ON M3J 1P3, Canada. Tel.: +1 416 736 2100×20452; fax: +1 416 736 5814.
*E-mail address:* steeves@yorku.ca (J.K.E. Steeves).

http://dx.doi.org/10.1016/j.nicl.2014.11.020

visual cortex in response to the loss of one eye early in life (reviewed in Kelly et al., 2013a; Steeves et al., 2008).

While behavioural visual development is well-documented following early eye enucleation, less is understood regarding the long-term consequences on the morphological development of the visual system in adult humans. Subcortically, non-primate models of enucleation show increased crossed retinal projections from the remaining eye in mice and rabbits (Grigonis et al., 1986; Godement et al., 1987), and rabbits exhibit a 50% reduction in volume of the deafferented LGN (Grigonis et al., 1986). Cortically, early eye-enucleated mice display an expansion and accelerated refinement of retinotopic primary visual cortex (V1) (Faguet et al., 2009), as well as decreased neuronal density and metabolic activity in visual cortex contralateral to the enucleated eye (Heumann and Rabinowicz, 1982; Chow et al., 2011). In monkeys, postnatal monocular enucleation is associated with cell degeneration, and a reduction in or lack of LGN layers and ocular dominance columns in V1 associated with the enucleated eye (Rakic, 1981; Sloper et al., 1987; Horton and Hocking, 1998).

Limited research has been conducted on the effects of eye enucleation on the morphology of the human visual system. The majority of these studies consist of post-mortem brains of adults who lost an eye during adulthood when the critical period for development has long been surpassed (Beatty et al., 1982; Horton, 1997; Adams et al., 2007). A handful of studies have assessed early enucleation in children and found results similar to monkey models of enucleation (Rakic, 1981; Sloper et al., 1987; Horton and Hocking, 1998); yet, these studies were conducted post-mortem on children whose visual system had not yet reached maturity. For example, one study showed that enucleation at 6 years of age resulted in degenerated LGN layers (Hickey and Guillery, 1979). Another study found a lack of ocular dominance columns in two children enucleated in infancy due to retinoblastoma (Horton & Hocking, 1998). One child had tumors in the remaining eye, resulting in decreased acuity, and both children died from brain tumors that may have affected cortical development independent of the enucleated eye. Physiologically, children who have been enucleated early in life have stronger functional activity in V1 contralateral to the remaining eye (Barb et al., 2011). These data suggest that the lack of binocular competition for space within visual cortex alters the development of primary visual cortex.

Previous studies of enucleation fail to address whether the changes observed in childhood persist throughout adulthood, or whether the visual system continues to change past the age of maturity. To answer this question, we have previously conducted a study assessing subcortical development following early monocular enucleation in adults (Kelly et al., 2014a). Using structural magnetic resonance imaging (MRI), we examined optic nerve and optic tract widths, and optic chiasm and LGN volumes. We found that the early enucleation group exhibited general decreases in the structures observed compared with binocularly intact controls. A surprising finding, however, was that decreases in optic tract width and LGN volume were less severe contralateral to the remaining eye. This asymmetry points to a relative sparing of geniculate cells contralateral to the remaining eye, which may be attributed to recruitment of deafferented cells by crossing retinal fibres and/or feedback from ipsilateral V1 with early eye enucleation. This notion is supported by rabbit and monkey models of enucleation showing that aberrant connections are formed between the remaining intact eye and deafferented geniculate cells (Rakic, 1981; Grigonis et al., 1986).

The goal of the present study was to expand on the subcortical data found in our laboratory and to determine how the visual cortex develops morphologically following long-term survival from early eye enucleation. We used structural MRI to assess surface area, thickness, and gyrification of the cortical grey matter in a group of individuals who experienced early monocular enucleation due to retinoblastoma and compared their results to binocularly intact controls. These morphological measures have been previously used to assess developmental disorders affecting vision, such as congenital anophthalmia (Bridge et al., 2009) and congenital blindness (Jiang et al., 2009; Park et al., 2009). We conducted: 1) whole brain analyses to examine regional differences across the entire cortical surface, 2) region-of-interest (ROI) analyses to examine differences in early visual regions known to process spatial form vision (V1, V2) (e.g., Hubel and Livingstone, 1987; Tootell et al., 1988), and 3) correlations with age at enucleation to examine the effect of timing of deprivation on these measures. Since cortical changes have been observed in non-primate and non-human primate models of early enucleation, and in human studies examining other forms of early visual deprivation (i.e., strabismus, amblyopia), we expect to observe altered morphological development of the visual cortex in the adult human brain following long-term survival from early monocular enucleation. In particular, we predict that enucleation will be associated with morphological changes in early visual areas V1 and V2. We also expect to observe hemisphere asymmetries in early visual cortices, similar to the contralateral biases found for LGN volume (Kelly et al., 2014a) and cortical activity in V1 of early-enucleated children (Barb et al., 2011). Findings from this study will help elucidate the effects of early monocular enucleation on long-term, morphological visual development, and will provide insight into the requirements for typical visual system maturation.

## 2. Methods

### 2.1. Participants

#### 2.1.1. Early monocular enucleation (ME) group

We tested a rare group of 9 adults (5 males) who were former patients at The Hospital for Sick Children in Toronto, and had their right eye enucleated early in life due to retinoblastoma. Mean age (±SD) was 26 ± 14 years (range = 17–54 years) and mean age at enucleation (AAE) (±SD) was 20 ± 13 months (range = 4–48 months). Based on the size and position of the tumour under retinal examination, it is estimated that the average tumour would have disrupted vision approximately 6 months prior to enucleation. All participants had normal or corrected-to-normal acuity as assessed by an EDTRS eye chart (Precision Vision™, La Salle, IL). Patients are regularly seen by their ophthalmologist, and no known neurological or ocular abnormalities in the remaining eye were reported (Table 1 lists individual patient histories). Based on our previous study showing an LGN asymmetry in early enucleation (Kelly et al., 2014a), and the fact that we were unable to recruit a sufficient number of left-eye enucleated participants due to the rarity of these patients, we restricted our analyses to right eye-enucleated participants only.

#### 2.1.2. Control group

Eighteen binocularly intact controls (10 males) were tested who were approximately age- and sex-matched to the early ME group. Mean age (±SD) was 28 ± 12 years (range = 18–57 years). Participants had normal or corrected-to-normal acuity (Precision Vision™,

**Table 1**
Patient histories for ME participants including age, sex, Snellen acuity, enucleated eye, and age at enucleation (AAE).

| Patient | Age (years) | Sex | Acuity | Enucleated Eye | AAE (months) |
|---|---|---|---|---|---|
| ME01 | 54 | Male | 20/16 − 1 | Right | 24 |
| ME02 | 43 | Female | 20/12.5 + 2 | Right | 18 |
| ME03 | 21 | Male | 20/20 | Right | 23 |
| ME04 | 18 | Female | 20/20 | Right | 48 |
| ME05 | 18 | Male | 20/20 + 4 | Right | 13 |
| ME06 | 17 | Male | 20/20 + 2 | Right | 9 |
| ME07 | 28 | Male | 20/16 | Right | 4 |
| ME08 | 18 | Female | 20/16 + 3 | Right | 17 |
| ME09 | 17 | Female | 20/12.5 + 1 | Right | 26 |

La Salle, IL) and normal Titmus stereoacuity (Stereo Optical Co., Inc., Chicago, IL).

### 2.2. MRI data acquisition

This research followed the Declaration of Helsinki doctrine and was approved by the Research Ethics Boards of both The Hospital for Sick Children and York University. Informed consent was obtained from all participants prior to testing and after explanation of the nature and possible consequences of the study.

A high resolution, $T_1$ weighted three-dimensional MPRAGE anatomical image was obtained for all participants using a Siemens MAGNETOM Tim Trio 3 T MRI scanner with a 32-channel head coil at the Sherman Health Sciences Research Centre at York University (Toronto, Canada). A scan of the entire head was acquired sagittally with the following parameters: rapid gradient echo, 1 $mm^3$ isotropic voxels, TR = 1900 ms, TE = 2.52 ms, 256 × 256 matrix, and flip angle = 9°.

### 2.3. Surface-based morphometry

Each $T_1$ weighted image was processed using the surface-based registration pipeline in the FreeSurfer (version 5.3) image analysis suite (http://surfer.nmr.mgh.harvard.edu/). This fully automated process has been previously described (Dale et al., 1999; Fischl and Dale, 2000), and briefly includes: Talairach transformation, motion correction, intensity normalization, removal of non-brain tissue, segmentation and tessellation of the grey and white matter boundary, automatic topology correction, and surface deformation. Given that there is a one-to-one correspondence of points on the white matter surface to the pial matter surface, the grey matter–white matter boundary was then used as an initial contour that deformed to detect the grey matter-pial matter boundary with subvoxel precision (Fischl and Dale, 2000). This procedure has been validated against histological analysis (Rosas et al., 2002) and manual measurements (Salat et al., 2004). Reconstructed surfaces were visually evaluated for errors in Talairach registration, brain extraction, and segmentation, and minimal manual editing was performed when necessary.

Following surface reconstruction, estimates of surface area, cortical thickness, and gyrification were derived from the native space of each participant. Surface area was calculated by estimating the relative areal expansion or compression at each vertex on the tessellated surface of the pial matter. In anatomical regions-of-interest (ROIs), surface area was calculated as the sum of each vertex in a given ROI. Cortical thickness was calculated as the average of the shortest distance between the white matter to pial matter surface and from the pial matter to white matter surface at each vertex on the tessellated surface. Gyrification was measured as a local gyrification index (LGI) using an automated method available in FreeSurfer (Schaer et al., 2012). The LGI measure is a ratio of the amount of cortex buried in sulcal folds compared with the amount of cortex on the outer visible surface (i.e., sulcal depth). Large LGIs denote extensive folding whereas small LGIs denote limited folding. To ensure that whole brain volume was not a factor affecting our results, volumetric segmentation was also performed with FreeSurfer to calculate whole brain volumes per participant excluding the cerebellum and brain stem.

### 2.4. Data analyses

#### 2.4.1. Whole brain volume and global differences

An independent *t*-test was performed to determine group differences in whole brain volume. Global morphometry differences in surface area, cortical thickness, and gyrification of the entire cortical grey matter surface were assessed using a 2 × 2 analysis of variance (ANOVA) with group (control, early ME) as the between-groups variable, and hemisphere (left, right) as the within-groups variable. Post-hoc pairwise comparisons were conducted on significant ANOVAs.

#### 2.4.2. Regional differences

Regional morphometry differences in surface area, cortical thickness, and gyrification of the entire cortical grey matter surface were assessed between groups using a vertex-by-vertex general linear model (GLM) conducted in FreeSurfer's GUI-based Qdec (Query, Design, Estimate, Contrast) application. Statistical analyses of surface area, cortical thickness, and gyrification were performed at 163,842 vertices per hemisphere. Cortical surfaces from each participant were transformed to an average template surface space that is provided by FreeSurfer and created in MNI305 space. Smoothing was applied at different surface-based Gaussian kernel values for each morphology measure map [full-width half medium (FWHM) = 10–20 mm]. For the main analyses and figures, FWHM values of 10 mm were used for cortical thickness and surface area and 20 mm for gyrification, given that the scale of differences is always greater for gyrification. Contiguous clusters of significant vertex-wise group differences were identified using a minimum cluster size of 50 $mm^2$ and an uncorrected $p < 0.001$ due to the small sample size of the enucleation group. Significant regions were identified according to FreeSurfer's implemented Desikan–Killiany–Tourville (DKT) atlas parcellation that segments the cortical surface into 40 labels based on gyral and sulcal structure (Klein and Tourville, 2012).

#### 2.4.3. Region-of-interest (ROI) differences

We restricted our ROI analysis of visual cortex to anatomical V1 and V2 labels, which are implemented in FreeSurfer's automatic processing stream and are based on cortical folding patterns corresponding to anatomical Brodmann areas 17 and 18, respectively. These labels have previously been validated (Fischl et al., 2008; Hinds et al., 2009) and used in studies assessing clinical populations known to display visual deficits [e.g., schizophrenia (Schultz et al., 2013), albinism (Bridge et al., 2014)]. These labels were mapped to each individual brain using a previously tested thresholded *p* level of 0.80 (Hinds et al., 2009). Total surface area, mean cortical thickness, and mean gyrification indices were calculated for each label and participant. Fig. 1 illustrates the topography of V1 and V2 in a typical control and typical early enucleation patient.

ROI morphometry differences were assessed using a series of 2 × 2 analysis of covariance (ANCOVAs) per hemisphere with group (control, early ME) as the between-groups variable, ROI (V1, V2) as the within-groups variables, and global morphometry measure as the covariate. Post-hoc pairwise comparisons were conducted on significant ANCOVAs.

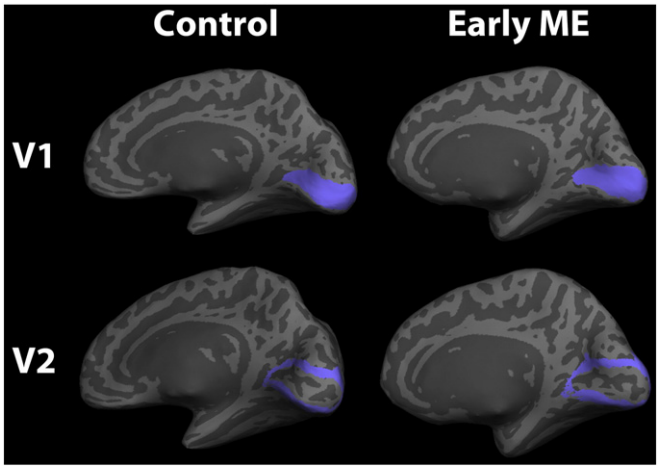


**Fig. 1.** V1 and V2 topography (blue) of the right hemisphere on an inflated surface for a typical control and early MR participants.

*2.4.4. Timing of deprivation*

Correlations controlling for sex and age were conducted for the entire cortical surface area on a vertex-by-vertex basis using Qdec to determine whether there was a relationship between AAE and any morphometry measure ($p < 0.05$, FDR-corrected). Partial correlations were also conducted on V1 and V2 ROIs controlling for sex and age to determine whether there was a relationship between AAE and any morphometry measure.

## 3. Results

There were no significant group differences in age ($p = 0.669$) or sex ($p = 0.660$). Therefore, age and sex were not factored into the analyses.

### 3.1. Whole brain volume and global differences

Whole brain volumes, and global estimates of surface area, cortical thickness and gyrification of the early ME and control groups were within the range previously reported for healthy controls (Allen et al., 2002; Ge et al., 2002; Van Essen et al., 2012; Hogstrom et al., 2013; Meyer et al., 2014) (see Table 2 for means [±standard error of the mean (SEM)] for whole brain volume and each global morphometry measure per group).

*3.1.1. Whole brain volume*

No significant group difference was found for whole brain volume, $t(25) = -0.36$, $p = 0.719$.

*3.1.2. Surface area*

No significant group × hemisphere interaction was found, $F(1,25) = 0.86$, $p = 0.362$. However, significant main effects of hemisphere, $F(1,25) = 351.42$, $p < 0.001$, and group, $F(1,25) = 4.87$, $p = 0.037$, were found. Global surface area was larger in the right compared with left hemisphere for both groups ($ps < 0.001$). Further, the early ME group exhibited significantly larger global surface area compared with the control group ($ps \leq 0.044$).

*3.1.3. Cortical thickness*

No significant group × hemisphere interaction, $F(1,25) = 0.56$, $p = 0.461$, or main effect of group, $F(1,25) = 1.74$, $p = 0.199$, were found. However, there was a significant main effect of hemisphere, $F(1,25) = 4.60$, $p = 0.042$. There was a trend for the early ME group to exhibit larger global cortical thickness in the left compared with right hemisphere; however, this trend was not significant ($p = 0.089$).

*3.1.4. Gyrification*

No significant group × hemisphere interaction, $F(1,25) = 0.84$, $p = 0.367$, or main effect of hemisphere, $F(1,25) = 0.14$, $p = 0.710$, was found. However, there was a significant main effect of group, $F(1,25) = 9.53$, $p = 0.005$. The early ME group exhibited significantly larger global gyrification compared with the control group in both hemispheres ($ps = 0.006$).

### 3.2. Regional differences

*3.2.1. Surface area*

Four main clusters were flagged as significantly larger in surface area in the early ME compared with the control group ($p < 0.001$). These clusters were located in right inferior temporal, and left supramarginal, superior temporal, and superior parietal regions (see Fig. 2A and Table 3).

*3.2.2. Cortical thickness*

No significant regional group differences were found for cortical thickness in either hemisphere.

*3.2.3. Gyrification*

Three main clusters were flagged as significantly larger in the early ME group compared with controls. These clusters were located in right inferior temporal and superior parietal, and left inferior parietal regions ($p < 0.001$) (see Fig. 2B and Table 3).

### 3.3. Region-of-interest (ROI) differences

Surface area, cortical thickness, and gyrification estimates for V1 and V2 in the control group were within the range previously reported for healthy controls (Stensaas et al., 1974; Hinds et al., 2009; Hogstrom et al., 2013). Significant results were only found for surface area, and thus, are the only ROI differences reported.

For the right hemisphere, no significant group × ROI interaction was found, $F(1,24) = 2.19$, $p = 0.152$. However, there was a trend towards a significant main effect of group, $F(1,24) = 3.90$, $p = 0.060$. Post hoc pairwise comparisons reveal that the early ME group exhibited significantly increased surface area in V1 ($p = 0.016$), but not in V2 ($p = 0.296$), compared to the control group. For the left hemisphere, no significant group × ROI interaction, $F(1,24) = 1.89$, $p = 0.182$, or main effect of group, $F(1,24) = 0.10$, $p = 0.761$, was found (see Fig. 3 and Inline Supplementary Table S1 for group averages of surface area per ROI).

Inline Supplementary Table S1 can be found online at http://dx.doi.org/10.1016/j.nicl.2014.11.020.

*3.3.4. Timing of deprivation*

No significant correlations were found between AAE and any morphometry measure for regional ($p > 0.05$) or ROI differences ($ps \geq 0.287$) for the early ME group.

## 4. Discussion

We report the first instance of morphological changes in human cortex following long-term survival from early monocular enucleation due to retinoblastoma. Compared to controls, the early enucleation group exhibited increases in surface area and gyrification in visual, auditory, and multisensory cortices. Further, increased surface area in visual regions was restricted to V1 and inferior temporal cortex, contralateral to the remaining eye. These differences are in line with subcortical data found in the same group (Kelly et al., 2014a), and show altered neural development following long-term survival subsequent to early monocular enucleation.

### 4.1. Visual cortices

As expected, we found that early enucleation results in morphological changes in visual cortex, and that these changes include increases, but not decreases, in morphology measures assessed in this study. The

**Table 2**
Descriptive statistics for the control and early ME groups showing mean (±SEM) whole brain volume and global estimates for surface area, cortical thickness and gyrification in the right and left hemisphere.

| Group | Whole brain volume ($cm^3$) | Surface area ($cm^2$) | | Cortical thickness (mm) | | Gyrification (LGI) | |
|---|---|---|---|---|---|---|---|
| | | Right | Left | Right | Left | Right | Left |
| Control | 1034 (28) | 1089 (27) | 1025 (26) | 2.57 (0.02) | 2.57 (0.02) | 2.89 (0.03) | 2.89 (0.02) |
| Early ME | 1051 (35) | 1186 (36) | 1128 (36) | 2.60 (0.03) | 2.62 (0.03) | 3.06 (0.05) | 3.04 (0.05) |

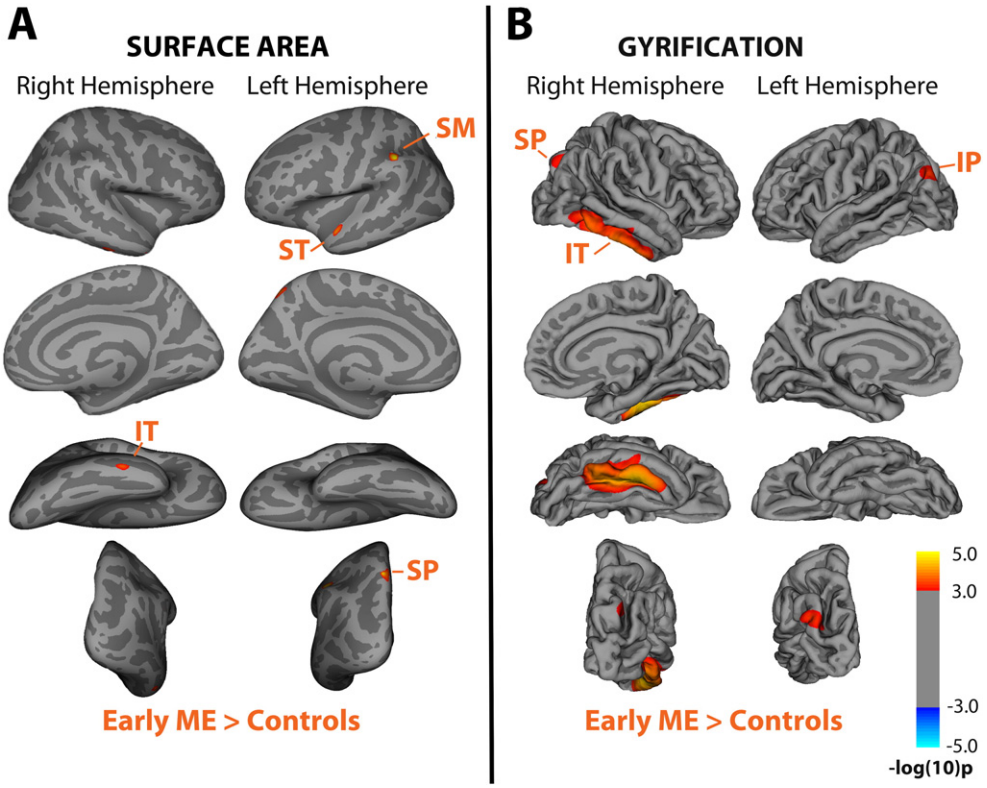


**Fig. 2.** Average inflated brain showing regions of increased (A) surface area and (B) gyrification in the right and left hemispheres in the early ME group compared to controls. (A) The early ME group exhibited significantly larger surface area compared with the control group in clusters located in right inferior temporal (IT), and left supramarginal (SM), superior temporal (ST), and superior parietal (SP) regions. (B) The early ME group also exhibited significantly increased gyrification compared with the control group in clusters located in right inferior temporal (IT) and superior parietal (SP), and left inferior parietal (IP) regions ($p < 0.001$).

increase in surface area in right V1 is inconsistent with decreased surface area in bilaterally enucleated monkeys (Rakic, 1988), and congenitally blind humans (Park et al., 2009). These discrepancies are expected given that the remaining intact eye in enucleated individuals allows one stream of normal visual input to the brain, unlike bilateral blindness. Increased surface area in V1 may explain the lack of spatial form vision deficits in the early eye-enucleated population (reviewed in Steeves et al., 2008; Kelly et al., 2013a), and is consistent with mouse models showing that early enucleation expands and accelerates the refinement of retinotopic area V1 (Smith and Trachtenberg, 2007; Faguet et al., 2009). V2, however, appears to be unaffected morphologically by early eye enucleation, which is in line with previous data showing a typical pattern of stripes within area V2 of early enucleated monkeys using cytochrome oxidase staining (Horton and Hocking, 1998).

Of importance is the finding that the surface area increase in V1 was restricted to the right hemisphere, contralateral to the remaining eye. The V1 asymmetry is consistent with our previous study showing a contralateral bias for LGN volume (Kelly et al., 2014a), and with behavioural studies showing a nasalward bias for motion processing (Steeves et al., 2002) in the early enucleation population. Monocularly enucleated children (Barb et al., 2011) and binocularly intact controls viewing monocularly (Toosy et al., 2001) exhibit a contralateral bias in functional activity in V1, suggesting that V1 receives stronger physiological inputs from the contralateral eye. In primates, the total retinal projection from the nasal hemiretina (~53–58%) is greater than the projection from temporal hemiretina (~47–42%), and binocularly intact monkeys have a greater contribution of crossed nasal retinal inputs to ocular dominance columns (Chacko, 1948; Kupfer et al., 1967; Horton, 1997; Tychsen and Burkhalter, 1997). Therefore, it is not that surprising that contralateral V1 cortex is more affected following enucleation.

One can argue that while we sought to examine anatomic V1, we did so without retinotopic identification. It is difficult to say whether the location of functional V1 in a visually deprived group is correlated well with the anatomical location based on folding patterns alone. While

**Table 3**
Information for clusters flagged as significantly larger in the early ME compared to the control group, including region, cluster size ($mm^2$), maximum $-\log(10)p$ value, and MNI coordinates.

| Measure | Hemisphere | Region | Cluster size ($mm^2$) | Max $-\log(10)p$ | MNI coordinates | | |
|---|---|---|---|---|---|---|---|
| | | | | | X | Y | Z |
| Surface area | Right | Inferior temporal | 84 | 3.6 | 57 | −26 | −25 |
| | Left | Supramarginal | 187 | 5.2 | −50 | −40 | 44 |
| | | Superior parietal | 185 | 4.7 | −11 | −70 | 52 |
| | | Superior temporal | 106 | 4.0 | −52 | 3 | −11 |
| Gyrification | Right | Inferior temporal | 3290 | 4.6 | 50 | −24 | −27 |
| | | Superior parietal | 212 | 3.2 | 25 | −76 | 37 |
| | Left | Inferior parietal | 399 | 3.4 | −37 | −77 | 29 |

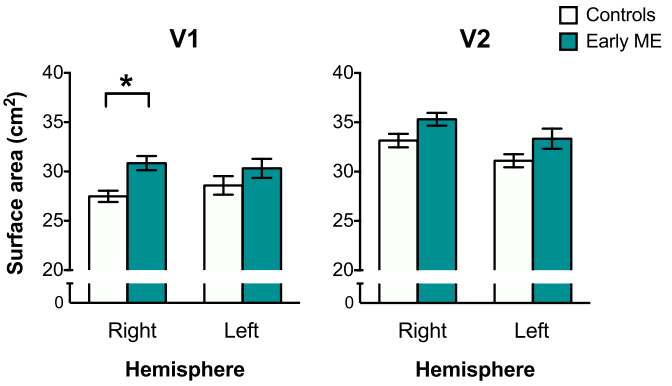


**Fig. 3.** Bar graphs depicting group averages for surface area ($cm^2$) for right and left V1 and V2 in the control (white) and early ME (blue) groups. The early ME group exhibited an increase in right V1 only compared to the control group. Error bars represent ±SEM. $^*p < 0.05$.

there is substantial individual variation in the size, volume, and position of V1 in the normal population, boundaries of V1 fall at a consistent locations across individuals when based on folding patterns of the cortical surface (Andrews et al., 1997; Amunts et al., 2000; Hinds et al., 2008; Benson et al., 2012). V1 and V2 labels available in FreeSurfer have been used to anatomically define these regions in other clinical populations known to exhibit visual deficits (i.e., albinism, schizophrenia) (Schultz et al., 2013; Bridge et al., 2014). Additionally, individuals with William's syndrome, a disorder known to result in visual impairments, exhibit more variation in the anatomical borders of V1 compared with controls; yet the size of V1 and the location of the centre of gravity (i.e., fundus of calcarine fissure) does not differ between the two groups (Olsen et al., 2009). While we cannot infer how these early visual regions develop physiologically following early monocular enucleation, we can be confident that the anatomical image alone can be used to predict the retinotopic organization of striate cortex in these individuals.

In line with a contralateral bias found for V1, the early ME group exhibited increased surface area and gyrification in inferior temporal cortex in the right (contralateral) hemisphere only. Inferior temporal cortex is associated with processing higher-level visual stimuli such as objects and faces (Kanwisher et al., 1997; Haxby et al., 2001). Recent research has revealed slower face processing and reduced activation in face regions following early monocular enucleation (Kelly et al., 2012; Kelly et al., 2014b). These findings may reflect alterations in morphology in face-selective regions during development. An increase in gyrification does not necessarily imply better performance on visual tasks, as is supported by our data and findings of increased gyrification in V1 of bilaterally enucleated monkeys (Rakic, 1988) and in lateral occipital complex in bilateral anophthalmia (Bridge et al., 2009). However, the previous finding of an increase in response times for behavioural face perception was coupled with accuracy comparable to controls, suggesting that the slower processing may be due to altered morphology, as is supported by the increase in surface area and gyrification in inferior temporal cortex in our study.

### 4.2. Possible mechanisms of altered development

Typical visual development is reliant upon the presence of activity-driven binocular interactions during postnatal maturation (Sloper, 1987, 1993). Ocular dominance columns are only partially segregated at birth and are thus more vulnerable to abnormal visual experience (Rakic, 1976; Sloper, 1993; Horton and Hocking, 1998). Binocular competition for cortical space in V1 during a time of rapid cortical development is lacking following monocular enucleation (for review see Steeves et al., 2008; Kelly et al., 2013a). Our study found that this lack of competition results in changes in the development of visual cortex. In the binocularly intact and monocularly enucleated visual system, V1 receives stronger inputs from the contralateral eye (Chacko, 1948; Kupfer et al., 1967; Horton, 1997; Tychsen and Burkhalter, 1997; Toosey et al., 2001; Barb et al., 2011), which may explain the asymmetry in surface area and gyrification in visual cortices observed in the enucleation group in our study. However, stronger contralateral inputs cannot be the sole determinant behind these changes and other factors must be considered. Here, we discuss other possible mechanisms behind the increases in surface area and gyrification that were found subsequent to early enucleation.

One possible explanation for the increases in surface area and gyrification in the early enucleation group is that due to the lack of binocular competition, the remaining eye may recruit deafferented cells within contralateral V1 while still developing (Rakic, 1981; Grigonis et al., 1986). This notion is not only supported by a lack of segregation of ocular dominance columns in early-enucleated monkeys and humans (Rakic, 1981; Horton and Hocking, 1998), but also by rabbit and monkey models of enucleation showing that aberrant connections are formed between the remaining intact eye and deafferented geniculate cells (Rakic, 1981; Grigonis et al., 1986). More cortical space in V1 devoted to the remaining eye would then affect development of visual areas beyond V1, which would also explain the surface area and gyrification increases observed for inferior temporal cortex. It could also be the case that feedback from extrastriate visual areas that have a larger proportion of binocular cells such as V2 may aid in the retention of cortical cells within V1. Indeed, inactivation of V2 in monkeys suppresses V1 neuron responses (Hupé et al., 2001). However, enucleation did not appear to affect morphological development of V2 in our study, which is consistent with monkey data showing that early enucleation does not affect staining within V2 (Horton and Hocking, 1998). Recruitment of deafferented cells may explain the asymmetry previously observed in the LGN, and could indeed explain why there is no decrease in surface area following enucleation. It is unlikely, though, that a recruitment of existing cells would lead to an increase in V1 or other cortical regions. unless recruited neurons hypertrophy as a result of the abnormal visual experience. For instance, enucleated monkeys exhibit hypertrophy of geniculate P cells (Sloper et al., 1987) and rabbits exhibit glial cell hyperplasia and hypertrophy in the LGN (Khan, 2005). It is possible that similar changes in these cells may also occur at the cortical level and could result in structural increases.

One could also argue that metabolic changes within cortex are behind the increases found in the enucleated group. Metabolic increases have been documented in the visual cortex contralateral to the enucleated eye in mice (Heumann and Rabinowicz, 1982; Chow et al., 2011), and at rest in congenitally blind individuals compared with sighted controls (Kupers et al., 2011). Our group of enucleated individuals is not blind and the pattern of stronger functional activation contralateral to the remaining eye within visual cortex is akin to binocular controls viewing monocularly (Toosy et al., 2001). Thus, metabolic increases are not likely to account for the increases observed in our group.

Synaptic pruning, gyrification, and myelination of the cortex continue until well into adolescence (Garey and De Courten, 1983; Magnotta et al., 1999; Barnea-Goraly et al., 2005; Gao et al., 2009; Klein et al., 2014). Differences in gyrification may indirectly reflect changes in connectivity of white matter, especially since the development of gyrification is closely related to the development of cortico-cortical connections. As white matter matures, fibres of the cortex are pulled or loosened based on the connections that are forming, which in turn changes the folding patterns of the cortex (Van Essen, 1997; Hilgetag and Barbas, 2006). Changes in the development of white matter connectivity following enucleation could result in altered gyrification. Since surface area is closely related to gyrification, this may also explain changes in surface area in the enucleation group. Feedback and feedforward connections between visual cortex and other sensory regions may drive changes in surface area and gyrification, which is

supported by increases in auditory and multisensory regions found in the enucleated group. No studies have assessed white matter integrity in this group, and future research should address this question.

Another plausible explanation for changes in morphology in our enucleation group is a disruption in synaptic pruning during development. This has also been put forth as an explanation for a similar finding in the congenitally blind (Park et al., 2009). Synaptogenesis typically is complete by 9 months of age (Garey and de Courten, 1983) and is followed by a period of synaptic pruning that continues until 11 years of age (Garey and De Courten, 1983; Huttenlocher and De Courten, 1987). Early enucleation in mice, ferrets, and rabbits results in increased contralateral retinogeniculate connections (Grigonis et al., 1986; Godement et al., 1987), suggesting disrupted pruning. A disruption in pruning may serve to reduce the instance of degeneration of visual neurons, and consequently spare visual function in a population whose brain is receiving only half of its typical visual input during development. However, increased thickness in congenital blindness is associated with decreased surface area (Park et al., 2009), which is inconsistent with our results. Therefore, it appears likely that different mechanisms are involved in the different forms of visual deprivation and we cannot say for certain that a lack of pruning is responsible for the morphological changes in our group.

Perhaps our most salient finding is that cortical thickness was unaffected by early enucleation. A variety of studies have shown that cortical thickness and surface area follow different developmental trajectories and are affected by different genetic characteristics and sensory experiences (Rakic, 1988; Fischl and Dale, 2000; Sowell, 2004; Panizzon et al., 2009; Rakic et al., 2009; Lyall et al., 2014). For example, one study found that between birth and 2 years of age, cortical thickness increases slowly and reaches adult levels by 2 years of age (Lyall et al., 2014). In stark contrast, surface area of the cortex increases rapidly but is still not at adult levels by 2 years of age. Other studies have found that surface area expands 2- to 4-fold between birth and adulthood (Hill et al., 2010) and peaks between 8 and 9 years of age (Raznahan et al., 2010). Therefore, the lack of cortical thickness changes in our study may be due to the fact that this measure is already established quite early in life. In the same vein, changes in surface area and gyrification may reflect the slower development of these measures that are more likely vulnerable to abnormal sensory experience. Further, surface area is well correlated with gyrification (e.g., Lyall et al., 2014), which may explain why we see somewhat similar patterns of results with these measures in the early enucleation group. Due to the limitations of structural neuroimaging techniques employed in this study, it is impossible to assess the cortex at a microscopic level to determine whether the observed cortical changes reflect changes in number and size of neurons, glial cells, synapses, or dendrites, or changes in myelin and white matter connections. Thus, future research must examine each of these possible mechanisms to gain more insight.

### 4.3. Non-visual cortices

Compared with controls, the early enucleation group exhibited increases in surface area and gyrification in regions not devoted solely to visual processing. These regions reside in superior parietal, inferior parietal, superior temporal, and supramarginal areas. The parietal cortex is implicated in visually-guided reaching (Faugier-Grimaud et al., 1985; Gallivan et al., 2009), an ability shown to be intact in early-enucleated individuals (Marotta et al., 1995). However, their strategies differ compared to binocularly intact controls as the enucleated group generated larger head movements (i.e., motion parallax) in order to perceive depth. The supramarginal gyrus, particularly in the left hemisphere, is considered the phonological store for short-term memory of auditory information, including language (Paulesu et al., 1993), and has been implicated in speech sound disorders (Tkach et al., 2011). The superior temporal sulcus has been implicated in audiovisual multisensory integration (Beauchamp et al., 2004). Increased surface area and gyrification for the early ME group in the supramarginal and superior temporal regions are consistent with previous behavioural research showing that early monocular enucleation results in moderately enhanced sound localization (Hoover et al., 2012), and equal reliance on visual and auditory information during audiovisual processing (Moro and Steeves, 2012, 2013). Morphological changes within these regions have also been observed in the congenitally blind (Park et al., 2009), a population who show superior hearing abilities for certain tasks such as sound localization (Lessard et al., 1998). Recruitment of other sensory and multisensory regions may serve as adaptive compensation during atypical visual development; however, future neuroimaging studies should correlate morphology and function in other sensory regions to fully ascertain whether these changes serve to compensate for the loss of one eye.

### 4.4. Timing of deprivation

No timing of deprivation effects were found for the early enucleation group, which is consistent with previous behavioural studies of spatial form vision (e.g., Steeves et al., 2004; Kelly et al., 2013b), and our previous structural LGN volume study (Kelly et al., 2014a). Unfortunately, we were unable to recruit more than one participant enucleated past the age of 4 years, which may be outside the developmental critical periods or may not span a sufficiently large range of time for developmental relationships to emerge. This is not surprising given synaptic pruning, gyrification, and myelination of the cortex is not complete until well into adolescence (Garey and De Courten, 1983; Magnotta et al., 1999; Barnea-Goraly et al., 2005; Gao et al., 2009; Klein et al., 2014). To address this concern, future studies should examine eye enucleation that has occurred later in life, preferably after 4 years of age, but before the visual system has reached adult levels (approximately 11 years of age) (Garey and De Courten, 1983).

Much of the previous research conducted on the structural effects of enucleation on the visual pathway has focused on late enucleation. However, enucleation late in life after the visual system has already matured would be expected to differ significantly from early enucleation when a young brain is still developing. Indeed, our previous LGN study (Kelly et al., 2014a) showed a different pattern of results in one late enucleate (age = 65 years) who lost his eye at 59 years of age due to trauma — while early enucleation resulted in an asymmetry in LGN volume, the late enucleate showed severe decreases in both LGN and no asymmetry. We did not have access to a group of late enucleates for the current study, but we were able to assess morphological measures in the one late enucleate from our previous LGN study. Similar to his LGN data, he exhibited bilateral decreases in cortical thickness and gyrification of V1 and V2, but no changes in surface area, compared to three age- and sex-matched controls (see Inline Supplementary Table S2). These data are in-line with other studies of late enucleation showing decreased ocular dominance columns associated with the enucleated eye (Adams et al., 2007).

Inline Supplementary Table S2 can be found online at http://dx.doi.org/10.1016/j.nicl.2014.11.020.

Changes in the early enucleation group are unlikely to be a result of the disease itself rather than the treatment (i.e., enucleation) that occurs during a time when the visual system is still maturing. Unilateral retinoblastoma is localized to the affected eye, is rarely associated with cancer in the other eye, and enucleation typically occurs immediately once the tumour is diagnosed before the cancer can extend beyond the eye. Thus, any effect that retinoblastoma has on the visual system is localized to the retinal ganglion cells at the tumour site prior to enucleation. Although we were unable to assess adults enucleated early in life due to circumstances other than retinoblastoma, such as trauma or infection, we would still expect to see similar results to those whom we have tested.

## 5. Conclusions

In conclusion, we report altered morphological cortical development subsequent to long-time survival from early eye loss. We observed increases in surface area and gyrification of visual, auditory, and multisensory regions. Further, the increase in visual cortex was restricted to the right hemisphere, indicating a contralateral bias that has previously been observed for geniculate volume, oculomotor function and behavioural motion abilities. These changes may reflect a number of possible mechanisms, including recruitment of deafferented cells by the remaining eye, a disruption in synaptic pruning, and disruption of white matter tract development.

## Funding

This research was funded by the Natural Sciences and Engineering Research Council of Canada (grant no. 327588), the Canada Foundation for Innovation (grant no. 12807), and the Canadian National Institute for the Blind.

## Acknowledgements

The authors would like to thank the monocular enucleation patients for their continuing participation in their studies. The authors would also like to thank Keith Schneider, Joy Williams and Aman Ish Goyal for their MRI acquisition and processing expertise.

## References

Adams, D.L., Sincich, L.C., Horton, J.C., 2007. Complete pattern of ocular dominance columns in human primary visual cortex. J. Neurosci. 27 (39), 10391–10403. http://dx.doi.org/10.1523/JNEUROSCI.2923-07.200717898211.

Allen, J.S., Damasio, H., Grabowski, T.J., 2002. Normal neuroanatomical variation in the human brain: an MRI-volumetric study. Am. J. Phys. Anthropol. 118 (4), 341–348. http://dx.doi.org/10.1002/ajpa.1009212124914.

Amunts, K., Malikovic, A., Mohlberg, H., Schormann, T., Zilles, K., 2000. Brodmann's areas 17 and 18 brought into stereotaxic space-where and how variable? Neuroimage 11 (1), 66–84. http://dx.doi.org/10.1006/nimg.1999.051610686118.

Andrews, T.J., Halpern, S.D., Purves, D., 1997. Correlated size variations in human visual cortex, lateral geniculate nucleus, and optic tract. J. Neurosci. 17 (8), 2859–28689092607.

Barb, S.M., Rodriguez-Galindo, C., Wilson, M.W., Phillips, N.S., Zou, P., Scoggins, M.A., Li, Y., Qaddoumi, I., Helton, K.J., Bikhazi, G., Haik, B.G., Ogg, R.J., 2011. Functional neuroimaging to characterize visual system development in children with retinoblastoma. Invest. Ophthalmol. Vis. Sci. 52 (5), 2619–2626. http://dx.doi.org/10.1167/iovs.10-560021245407.

Barnea-Goraly, N., Menon, V., Eckert, M., Tamm, L., Bammer, R., Karchemskiy, A., Dant, C.C., Reiss, A.L., 2005. White matter development during childhood and adolescence: a cross-sectional diffusion tensor imaging study. Cereb. Cortex 15 (12), 1848–1854. http://dx.doi.org/10.1093/cercor/bhi06215758200.

Barnes, G.R., Li, X., Thompson, B., Singh, K.D., Dumoulin, S.O., Hess, R.F., 2010. Decreased gray matter concentration in the lateral geniculate nuclei in human amblyopes. Invest. Ophthalmol. Vis. Sci. 51 (3), 1432–1438. http://dx.doi.org/10.1167/iovs.09-393119875650.

Beatty, R.M., Sadun, A.A., Smith, L., Vonsattel, J.P., Richardson, E.P., 1982. Direct demonstration of transsynaptic degeneration in the human visual system: a comparison of retrograde and anterograde changes. J. Neurol. Neurosurg. Psychiatry 45 (2), 143–146. http://dx.doi.org/10.1136/jnnp.45.2.1437069426.

Beauchamp, M.S., Lee, K.E., Argall, B.D., Martin, A., 2004. Integration of auditory and visual information about objects in superior temporal sulcus. Neuron 41 (5), 809–823. http://dx.doi.org/10.1016/S0896-6273(04)00070-415003179.

Benson, N.C., Butt, O.H., Datta, R., Radoeva, P.D., Brainard, D.H., Aguirre, G.K., 2012. The retinotopic organization of striate cortex is well predicted by surface topology. Curr. Biol. 22 (21), 2081–2085. http://dx.doi.org/10.1016/j.cub.2012.09.01423041195.

Bridge, H., Cowey, A., Ragge, N., Watkins, K., 2009. Imaging studies in congenital anophthalmia reveal preservation of brain architecture in "visual" cortex. Brain 132 (12), 3467–3480. http://dx.doi.org/10.1093/brain/awp27919892766.

Bridge, H., von dem Hagen, E.A., Davies, G., Chambers, C., Gouws, A., Hoffmann, M., Morland, A.B., 2014. Changes in brain morphology in albinism reflect reduced visual acuity. Cortex 56, 64–72. http://dx.doi.org/10.1016/j.cortex.2012.08.01023039995.

Broaddus, E., Topham, A., Singh, A.D., 2009a. Incidence of retinoblastoma in the USA: 1975–2004. Br. J. Ophthalmol. 93 (1), 21–23. http://dx.doi.org/10.1136/bjo.2008.13875018621794.

Broaddus, E., Topham, A., Singh, A.D., 2009b. Survival with retinoblastoma in the USA: 1975–2004. Br. J. Ophthalmol. 93 (1), 24–27. http://dx.doi.org/10.1136/bjo.2008.14384218718969.

Chacko, L.W., 1948. The laminar pattern of the lateral geniculate body in the primates. J. Neurol. Neurosurg. Psychiatry 11 (3), 211–224. http://dx.doi.org/10.1136/jnnp.11.3.21118878026.

Chow, A.M., Zhou, I.Y., Fan, S.J., Chan, K.W., Chan, K.C., Wu, E.X., 2011. Metabolic changes in visual cortex of neonatal monocular enucleated rat: a proton magnetic resonance spectroscopy study. Int. J. Dev. Neurosci. 29 (1), 25–30. http://dx.doi.org/10.1016/j.ijdevneu.2010.10.00220950681.

Dale, A.M., Fischl, B., Sereno, M.I., 1999. Cortical surface-based analysis. I. Segmentation and surface reconstruction. Neuroimage 9 (2), 179–194. http://dx.doi.org/10.1006/nimg.1998.03959931268.

Daw, N.W., 2006. Visual Development second edition. Springer, New York (NY).

Ellemberg, D., Lewis, T.L., Maurer, D., Brent, H.P., 2000. Influence of monocular deprivation during infancy on the later development of spatial and temporal vision. Vision Res. 40 (23), 3283–3295. http://dx.doi.org/10.1016/S0042-6989(00)00165-611008144.

Faguet, J., Maranhao, B., Smith, S.L., Trachtenberg, J.T., 2009. Ipsilateral eye cortical maps are uniquely sensitive to binocular plasticity. J. Neurophysiol. 101 (2), 855–861. http://dx.doi.org/10.1152/jn.90893.200819052109.

Faugier-Grimaud, S., Frenois, C., Peronnet, F., 1985. Effects of posterior parietal lesions on visually guided movements in monkeys. Exp. Brain Res. 59 (1), 125–138. http://dx.doi.org/10.1007/BF002376734018192.

Fischl, B., Dale, A.M., 2000. Measuring the thickness of the human cerebral cortex from magnetic resonance images. Proc. Natl. Acad. Sci. U S A. 97 (20), 11050–11055. http://dx.doi.org/10.1073/pnas.20003379710984517.

Fischl, B., Rajendran, N., Busa, E., Augustinack, J., Hinds, O., Yeo, B.T., Mohlberg, H., Amunts, K., Zilles, K., 2008. Cortical folding patterns and predicting cytoarchitecture. Cereb. Cortex 18 (8), 1973–1980. http://dx.doi.org/10.1093/cercor/bhm22518079129.

Gallivan, J.P., Cavina-Pratesi, C., Culham, J.C., 2009. Is that within reach? fMRI reveals that the human superior parieto-occipital cortex encodes objects reachable by the hand. J. Neurosci. 29 (14), 4381–4391. http://dx.doi.org/10.1523/JNEUROSCI.0377-09.200919357266.

Gao, W., Lin, W., Chen, Y., Gerig, G., Smith, J.K., Jewells, V., Gilmore, J.H., 2009. Temporal and spatial development of axonal maturation and myelination of white matter in the developing brain. A.J.N.R. Am. J. Neuroradiol. 30 (2), 290–296. http://dx.doi.org/10.3174/ajnr.A136319001533.

Garey, L.J., de Courten, C., 1983. Structural development of the lateral geniculate nucleus and visual cortex in monkey and man. Behav. Brain Res. 10 (1), 3–13. http://dx.doi.org/10.1016/0166-4328(83)90145-66639728.

Ge, Y., Grossman, R.I., Babb, J.S., Rabin, M.L., Mannon, L.J., Kolson, D.L., 2002. Age-related total gray matter and white matter changes in normal adult brain. Part I: volumetric MR imaging analysis. A.J.N.R. Am. J. Neuroradiol. 23 (8), 1327–133312223373.

Godement, P., Salaün, J., Métin, C., 1987. Fate of uncrossed retinal projections following early or late prenatal monocular enucleation in the mouse. J. Comp. Neurol. 255 (1), 97–109. http://dx.doi.org/10.1002/cne.9025501083819012.

Grigonis, A.M., Pearson, H.E., Murphy, E.H., 1986. The effects of neonatal monocular enucleation on the organization of ipsilateral and contralateral retinothalamic projections in the rabbit. Brain Res. 394 (1), 9–19. http://dx.doi.org/10.1016/0165-3806(86)90077-53756534.

Haxby, J.V., Gobbini, M.I., Furey, M.L., Ishai, A., Schouten, J.L., Pietrini, P., 2001. Distributed and overlapping representations of faces and objects in ventral temporal cortex. Science 293 (5539), 2425–2430. http://dx.doi.org/10.1126/science.106373611577229.

Heumann, D., Rabinowicz, T., 1982. Postnatal development of the visual cortex of the mouse after enucleation at birth. Exp. Brain Res. 46 (1), 99–106. http://dx.doi.org/10.1007/BF002381037067792.

Hickey, T.L., Guillery, R.W., 1979. Variability of laminar patterns in the human lateral geniculate nucleus. J. Comp. Neurol. 183 (2), 221–246. http://dx.doi.org/10.1002/cne.901830202762256.

Hilgetag, C.C., Barbas, H., 2006. Role of mechanical factors in the morphology of the primate cerebral cortex. PLOS Comput. Biol. 2 (3), e22. http://dx.doi.org/10.1371/journal.pcbi.002002216557292.

Hill, J., Inder, T., Neil, J., Dierker, D., Harwell, J., Van Essen, D., 2010. Similar patterns of cortical expansion during human development and evolution. Proc. Natl. Acad. Sci. U S A. 107 (29), 13135–13140. http://dx.doi.org/10.1073/pnas.100122910720624964.

Hinds, O., Polimeni, J.R., Rajendran, N., Balasubramanian, M., Amunts, K., Zilles, K., Schwartz, E.L., Fischl, B., Triantafyllou, C., 2009. Locating the functional and anatomical boundaries of human primary visual cortex. Neuroimage 46 (4), 915–922. http://dx.doi.org/10.1016/j.neuroimage.2009.03.03619328238.

Hinds, O.P., Rajendran, N., Polimeni, J.R., Augustinack, J.C., Wiggins, G., Wald, L.L., Diana Rosas, H., Potthast, A., Schwartz, E.L., Fischl, B., 2008. Accurate prediction of V1 location from cortical folds in a surface coordinate system. Neuroimage 39 (4), 1585–1599. http://dx.doi.org/10.1016/j.neuroimage.2007.10.03318055222.

Hogstrom, L.J., Westlye, L.T., Walhovd, K.B., Fjell, A.M., 2013. The structure of the cerebral cortex across adult life: age-related patterns of surface area, thickness, and gyrification. Cereb. Cortex 23 (11), 2521–2530. http://dx.doi.org/10.1093/cercor/bhs23122892423.

Hoover, A.E., Harris, L.R., Steeves, J.K., 2012. Sensory compensation in sound localization in people with one eye. Exp. Brain Res. 216 (4), 565–574. http://dx.doi.org/10.1007/s00221-011-2960-022130779.

Horton, J.C., 1997. Wilbrand's knee of the primate optic chiasm is an artefact of monocular enucleation. Trans. Am. Ophthalmol. Soc. 95, 579–6099440188.

Horton, J.C., Hocking, D.R., 1998. Effect of early monocular enucleation upon ocular dominance columns and cytochrome oxidase activity in monkey and human visual cortex. Vis. Neurosci. 15 (2), 289–303. http://dx.doi.org/10.1017/S0952523898152124960553O.

Hubel, D.H., Livingstone, M.S., 1987. Segregation of form, color, and stereopsis in primate area 18. J. Neurosci. 7 (11), 3378–34152824714.

Hupé, J.M., James, A.C., Girard, P., Bullier, J., 2001. Response modulations by static texture surround in area V1 of the macaque monkey do not depend on feedback connections from V2. J. Neurophysiol. 85 (1), 146–16311152715.
Huttenlocher, P.R., de Courten, C., 1987. The development of synapses in striate cortex of man. Hum. Neurobiol. 6 (1), 1–93583840.
Jiang, J., Zhu, W., Shi, F., Liu, Y., Li, J., Qin, W., Li, K., Yu, C., Jiang, T., 2009. Thick visual cortex in the early blind. J. Neurosci. 29 (7), 2205–2211. http://dx.doi.org/10.1523/JNEUROSCI.5451-08.200919228973.
Kanwisher, N., McDermott, J., Chun, M.M., 1997. The fusiform face area: a module in human extrastriate cortex specialized for face perception. J. Neurosci. 17 (11), 4302–43119151747.
Kelly, K., Tcherassen, K., Gallie, B., Steeves, J., 2014b. Early monocular enucleation selectively disrupts the development of neural mechanisms for face perception. Journal of Vision 14 (10), 696. http://dx.doi.org/10.1167/14.10.696.
Kelly, K.R., Gallie, B.L., Steeves, J.K., 2012. Impaired face processing in early monocular deprivation from enucleation. Optom. Vis. Sci. 89 (2), 137–147. http://dx.doi.org/10.1097/OPX.0b013e318240488e22198795.
Kelly, K.R., McKetton, L., Schneider, K.A., Gallie, B.L., Steeves, J.K., 2014a. Altered anterior visual system development following early monocular enucleation. Neuroimage Clin. 4, 72–81. http://dx.doi.org/10.1016/j.nicl.2013.10.01424319655.
Kelly, K.R., Moro, S.S., Steeves, J.K.E., 2013a. Living with one eye: plasticity in visual and auditory systems. In: Steeves, J.K.E., Harris, L.R. (Eds.), Plasticity in Sensory Systems. Cambridge University Press, New York (NY), pp. 225–244.
Kelly, K.R., Zohar, S.R., Gallie, B.L., Steeves, J.K., 2013b. Impaired speed perception but intact luminance contrast perception in people with one eye. Invest. Ophthalmol. Vis. Sci. 54 (4), 3058–3064. http://dx.doi.org/10.1167/iovs.12-1118923557735.
Khan, A.A., 2005. Effects of monocular enucleation on the lateral geniculate nucleus (LGN) of rabbit: a qualitative light and electron microscopic study. Biol. Res. 16, 1–5.
Klein, A., Tourville, J., 2012. 101 labeled brain images and a consistent human cortical labeling protocol. Front. Neurosci. 6, 171. http://dx.doi.org/10.3389/fnins.2012.0017123227001.
Klein, D., Rotarska-Jagiela, A., Genc, E., Sritharan, S., Mohr, H., Roux, F., Han, C.E., Kaiser, M., Singer, W., Uhlhaas, P.J., 2014. Adolescent brain maturation and cortical folding: evidence for reductions in gyrification. P.L.O.S. ONE 9 (1), e84914. http://dx.doi.org/10.1371/journal.pone.008491424454765.
Kupers, R., Pietrini, P., Ricciardi, E., Ptito, M., 2011. The nature of consciousness in the visually deprived brain. Front. Psychol. 2, 19. http://dx.doi.org/10.3389/fpsyg.2011.0001921713178.
Kupfer, C., Chumbley, L., Downer, J.C., 1967. Quantitative histology of optic nerve, optic tract and lateral geniculate nucleus of man. J. Anat. 101 (3), 393–4016051727.
Lessard, N., Paré, M., Lepore, F., Lassonde, M., 1998. Early-blind human subjects localize sound sources better than sighted subjects. Nature 395 (6699), 278–280. http://dx.doi.org/10.1038/262289751055.
Lyall, A.E., Shi, F., Geng, X., Woolson, S., Li, G., Wang, L., Hamer, R.M., Shen, D., Gilmore, J.H., 2014. Dynamic development of regional cortical thickness and surface area in early childhood. Cereb. Cortex http://dx.doi.org/10.1093/cercor/bhu02724591525.
Magnotta, V.A., Andreasen, N.C., Schultz, S.K., Harris, G., Cizadlo, T., Heckel, D., Nopoulos, P., Flaum, M., 1999. Quantitative in vivo measurement of gyrification in the human brain: changes associated with aging. Cereb. Cortex 9 (2), 151–160. http://dx.doi.org/10.1093/cercor/9.2.15110220227.
Marotta, J.J., Perrot, T.S., Nicolle, D., Servos, P., Goodale, M.A., 1995. Adapting to monocular vision: grasping with one eye. Exp. Brain Res. 104 (1), 107–114. http://dx.doi.org/10.1007/BF002298607621928.
Mendola, J.D., Conner, I.P., Roy, A., Chan, S.T., Schwartz, T.L., Odom, J.V., Kwong, K.K., 2005. Voxel-based analysis of MRI detects abnormal visual cortex in children and adults with amblyopia. Hum Brain Mapp 25 (2), 222–236. http://dx.doi.org/10.1002/hbm.2010915846772.
Meyer, M., Liem, F., Hirsiger, S., Jäncke, L., Hänggi, J., 2014. Cortical surface area and cortical thickness demonstrate differential structural asymmetry in auditory-related areas of the human cortex. Cereb. Cortex 24 (10), 2541–2552. http://dx.doi.org/10.1093/cercor/bht09423645712.
Moro, S.S., Steeves, J.K., 2012. No Colavita effect: equal auditory and visual processing in people with one eye. Exp. Brain Res. 216 (3), 367–373. http://dx.doi.org/10.1007/s00221-011-2940-422105335.
Moro, S.S., Steeves, J.K., 2013. No Colavita effect: increasing temporal load maintains equal auditory and visual processing in people with one eye. Neurosci. Lett. 556, 186–190. http://dx.doi.org/10.1016/j.neulet.2013.09.06424103371.
Nicholas, J.J., Heywood, C.A., Cowey, A., 1996. Contrast sensitivity in one-eyed subjects. Vision Res. 36 (1), 175–180. http://dx.doi.org/10.1016/0042-6989(95)00119-K8746251.
Olsen, R.K., Kippenhan, J.S., Japee, S., Kohn, P., Mervis, C.B., Saad, Z.S., Morris, C.A., Meyer-Lindenberg, A., Berman, K.F., 2009. Retinotopically defined primary visual cortex in Williams syndrome. Brain 132 (3), 635–644. http://dx.doi.org/10.1093/brain/awn36219255058.
Panizzon, M.S., Fennema-Notestine, C., Eyler, L.T., Jernigan, T.L., Prom-Wormley, E., Neale, M., Jacobson, K., Lyons, M.J., Grant, M.D., Franz, C.E., et al., 2009. Distinct genetic influences on cortical surface area and cortical thickness. Cereb. Cortex 19 (11), 2728–2735. http://dx.doi.org/10.1093/cercor/bhp02619299253.
Park, H.-J., Lee, J.D., Kim, E.Y., Park, B., Oh, M.-K., Lee, S., Kim, J.J., 2009. Morphological alterations in the congenital blind based on the analysis of cortical thickness and surface area. Neuroimage 47 (1), 98–106. http://dx.doi.org/10.1016/j.neuroimage.2009.03.07619361567.
Paulesu, E., Frith, C.D., Frackowiak, R.S., 1993. The neural correlates of the verbal component of working memory. Nature 362 (6418), 342–345. http://dx.doi.org/10.1038/362342a08455719.
Rakic, P., 1976. Prenatal genesis of connections subserving ocular dominance in the rhesus monkey. Nature 261 (5560), 467–471. http://dx.doi.org/10.1038/261467a0819835.
Rakic, P., 1981. Development of visual centers in the primate brain depends on binocular competition before birth. Science 214 (4523), 928–931. http://dx.doi.org/10.1126/science.73025697302569.
Rakic, P., 1988. Specification of cerebral cortical areas. Science 241 (4862), 170–176. http://dx.doi.org/10.1126/science.32911163291116.
Rakic, P., 2009. Evolution of the neocortex: a perspective from developmental biology. Nat. Rev. Neurosci. 10 (10), 724–735. http://dx.doi.org/10.1038/nrn2719197631O5.
Raznahan, A., Lee, Y., Stidd, R., Long, R., Greenstein, D., Clasen, L., Addington, A., Gogtay, N., Rapoport, J.L., Giedd, J.N., 2010. Longitudinally mapping the influence of sex and androgen signaling on the dynamics of human cortical maturation in adolescence. Proc. Natl. Acad. Sci. U. S. A. 107 (39), 16988–16993. http://dx.doi.org/10.1073/pnas.1006025107204841422.
Reed, M.J., Steinbach, M.J., Anstis, S.M., Gallie, B., Smith, D., Kraft, S., 1991. The development of optokinetic nystagmus in strabismic and monocularly enucleated subjects. Behav. Brain Res. 46 (1), 31–42. http://dx.doi.org/10.1016/S0166-4328(05)80094-41786112.
Rosas, H.D., Liu, A.K., Hersch, S., Glessner, M., Ferrante, R.J., Salat, D.H., van der Kouwe, A., Jenkins, B.G., Dale, A.M., Fischl, B., 2002. Regional and progressive thinning of the cortical ribbon in Huntington's disease. Neurology 58 (5), 695–701. http://dx.doi.org/10.1212/WNL.58.5.69511889230.
Salat, D.H., Buckner, R.L., Snyder, A.Z., Greve, D.N., Desikan, R.S., Busa, E., Morris, J.C., Dale, A.M., Fischl, B., 2004. Thinning of the cerebral cortex in aging. Cereb. Cortex 14 (7), 721–730. http://dx.doi.org/10.1093/cercor/bhh03215054051.
Schaer, M., Cuadra, M.B., Schmansky, N., Fischl, B., Thiran, J.P., Eliez, S., 2012. How to measure cortical folding from MR images: a step-by-step tutorial to compute local gyrification index. J. Vis. Exp. 59 (59), e3417. http://dx.doi.org/10.3791/341722230945.
Schultz, C.C., Wagner, G., Koch, K., Gaser, C., Roebel, M., Schachtzabel, C., Nenadic, I., Reichenbach, J.R., Sauer, H., Schlösser, R.G., 2013. The visual cortex in schizophrenia: alterations of gyrification rather than cortical thickness — a combined cortical shape analysis. Brain Struct. Funct. 218 (1), 51–58. http://dx.doi.org/10.1007/s00429-011-0374-122200883.
Sloper, J.J., 1993. Edridge–Green lecture. Competition and cooperation in visual development. Eye (Lond) 7 (3), 319–331. http://dx.doi.org/10.1038/eye.1993.708224286.
Sloper, J.J., Headon, M.P., Powell, T.P., 1987. Effects of enucleation at different ages on the sizes of neurons in the lateral geniculate nucleus of infant and adult monkeys. Brain Res. 428 (2), 259–265. http://dx.doi.org/10.1016/0165-3806(87)90123-43828833.
Smith, S.L., Trachtenberg, J.T., 2007. Experience-dependent binocular competition in the visual cortex begins at eye opening. Nat Neurosci. 10 (3), 370–375.
Sowell, E.R., Thompson, P.M., Leonard, C.M., Welcome, S.E., Kan, E., Toga, A.W., 2004. Longitudinal mapping of cortical thickness and brain growth in normal children. J. Neurosci. 24 (38), 8223–8231. http://dx.doi.org/10.1523/JNEUROSCI.1798-04.200415385605.
Steeves, J.K., González, E.G., Gallie, B.L., Steinbach, M.J., 2002. Early unilateral enucleation disrupts motion processing. Vision Res. 42 (1), 143–150. http://dx.doi.org/10.1016/S0042-6989(01)00270-X11804638.
Steeves, J.K., González, E.G., Steinbach, M.J., 2008. Vision with one eye: a review of visual function following unilateral enucleation. Spat. Vis. 21 (6), 509–529. http://dx.doi.org/10.1163/156856808786451426190174480.
Steeves, J.K., Wilkinson, F., González, E.G., Wilson, H.R., Steinbach, M.J., 2004. Global shape discrimination at reduced contrast in enucleated observers. Vision Res. 44 (9), 943–949. http://dx.doi.org/10.1016/j.visres.2003.11.01514992838.
Stensaas, S.S., Eddington, D.K., Dobelle, W.H., 1974. The topography and variability of the primary visual cortex in man. J. Neurosurg. 40 (6), 747–755. http://dx.doi.org/10.3171/jns.1974.40.6.07474826600.
Tkach, J.A., Chen, X., Freebairn, L.A., Schmithorst, V.J., Holland, S.K., Lewis, B.A., 2011. Neural correlates of phonological processing in speech sound disorder: a functional magnetic resonance imaging study. Brain Lang. 119 (1), 42–49. http://dx.doi.org/10.1016/j.bandl.2011.02.00221458852.
Toosy, A.T., Werring, D.J., Plant, G.T., Bullmore, E.T., Miller, D.H., Thompson, A.J., 2001. Asymmetrical activation of human visual cortex demonstrated by functional MRI with monocular stimulation. Neuroimage 14 (3), 632–641. http://dx.doi.org/10.1006/nimg.2001.085111506536.
Tootell, R.B., Hamilton, S.L., Switkes, E., 1988. Functional anatomy of macaque striate cortex. IV. Contrast and magno-parvo streams. J. Neurosci. 8 (5), 1594–16093367212.
Tychsen, L., Burkhalter, A., 1997. Nasotemporal asymmetries in V1: ocular dominance columns of infant, adult, and strabismic macaque monkeys. J. Comp. Neurol. 388 (1), 32–46. http://dx.doi.org/10.1002/(SICI)1096-9861(19971110)388:1<32::AID-CNE3>3.0.CO;2-P9364237.
Van Essen, D.C., 1997. A tension-based theory of morphogenesis and compact wiring in the central nervous system. Nature 385 (6614), 313–318. http://dx.doi.org/10.1038/385313a09002514.
Van Essen, D.C., Glasser, M.F., Dierker, D.L., Harwell, J., Coalson, T., 2012. Parcellations and hemispheric asymmetries of human cerebral cortex analyzed on surface-based atlases. Cereb. Cortex 22 (10), 2241–2262. http://dx.doi.org/10.1093/cercor/bhr29122047963.
Wiesel, T.N., Hubel, D.H., 1965. Comparison of the effects of unilateral and bilateral eye closure on cortical unit responses in kittens. J. Neurophysiol. 28 (6), 1029–10405883730.